JAIST Repository
https://dspace.jaist.ac.jp/

Title	Nutrition analysis by nanoparticle-assisted laser desorption/ionisation mass spectrometry
Author(s)	Sahashi, Yuko; Osaka, Issey; Taira, Shu
Citation	Food Chemistry, 123(3): 865-871
Issue Date	2010
Type	Journal Article
Text version	author
URL	http://hdl.handle.net/10119/9049
Rights	NOTICE: This is the author's version of a work accepted for publication by Elsevier. Yuko Sahashi, Issey Osaka and Shu Taira, Food Chemistry, 123(3), 2010, 865-871, http://dx.doi.org/10.1016/j.foodchem.2010.05.008
Description	

JAIST
JAPAN ADVANCED INSTITUTE OF SCIENCE AND TECHNOLOGY

Japan Advanced Institute of Science and Technology

Accepted Manuscript

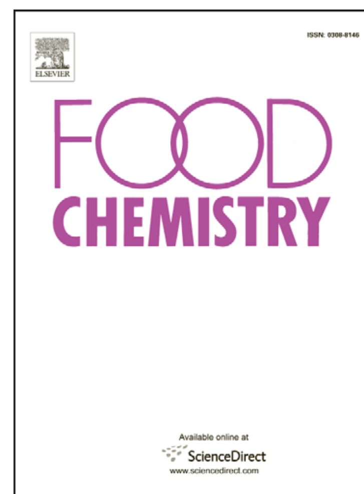

Nutrition analysis by nano-particle assisted laser desorption/ionization mass spectrometry

Yuko Sahashi, Issey Osaka, Shu Taira

PII: S0308-8146(10)00568-6
DOI: 10.1016/j.foodchem.2010.05.008
Reference: FOCH 9615

To appear in: *Food Chemistry*

Received Date: 19 November 2009
Revised Date: 25 March 2010
Accepted Date: 1 May 2010

Please cite this article as: Sahashi, Y., Osaka, I., Taira, S., Nutrition analysis by nano-particle assisted laser desorption/ionization mass spectrometry, *Food Chemistry* (2010), doi: 10.1016/j.foodchem.2010.05.008

This is a PDF file of an unedited manuscript that has been accepted for publication. As a service to our customers we are providing this early version of the manuscript. The manuscript will undergo copyediting, typesetting, and review of the resulting proof before it is published in its final form. Please note that during the production process errors may be discovered which could affect the content, and all legal disclaimers that apply to the journal pertain.

ACCEPTED MANUSCRIPT

1 Nutrition analysis by nano-particle assisted laser desorption/ionization mass
2 spectrometry.
3
4 Yuko Sahashi[1], Issey Osaka[2] and Shu Taira[3*]
5
6 [1] *Nitto Denko Corporation 1-1-2 Shimohozumi, Ibaraki, Osaka 567-8680, Japan*
7
8 [2] *Japan Advanced Institute of Science and Technology, Center for Nano Materials and*
9 *Technology, 1-1 Asahidai, Nomi, Ishikawa 923-1292, Japan*
10
11 [3] *Japan Advanced Institute of Science and Technology*
12 *School of Material Science 1-1 Asahidai, Nomi city, Ishikawa 923-1292, Japan*
13
14 [*]Corresponding author. e-mail: s-taira@jaist.ac.jp
15

ACCEPTED MANUSCRIPT

ACCEPTED MANUSCRIPT

16 Abstract

17 We analyzed the bioactive compounds in *Panax ginseng* C.A. Meyer by using
18 nanoparticle-assisted laser desorption/ionization (nano-PALDI) mass spectrometry (MS).
19 To this end, we prepared manganese oxide nanoparticles (d = 5.4 nm) and developed a
20 nano-PALDI MS method to analyze the standard ginsenosides and identify these
21 ginsenosides in an extract of *Panax ginseng*. The nanoparticles served as an
22 ionization-assisting reagent in MS. The mass spectra did not show any background
23 interference in the low-*m/z* range. Our pilot study showed that the nanoparticles could
24 ionize the standard ginsenosides and also respective lipid and ginsenosides in the extract
25 without the aid of chemical and liquid matrices used in conventional MS methods.
26 Analysis of the post-source decay spectra obtained using nano-PALDI MS will yield
27 information regarding the chemical structure of the analyte.

ACCEPTED MANUSCRIPT

ACCEPTED MANUSCRIPT

28 **Introduction**

29 Herbal products have been used in traditional Chinese medicine (TCM) for a
30 long time and have recently gained attention as complementary and alternative
31 medicines (Hijikata, Miyamae, Takatsu & Sentoh, 2007; Sun et al., 2009; Xu & Xu,
32 2009). *Panax ginseng* C.A. Meyer is one of the most famous oriental herbs used in
33 TCM, and it contains many bioactive compounds, including triterpene glycosides called
34 ginsenosides. Although ginsenosides have been thought to be the main bioactive
35 components in *Panax ginseng* (Metori, Furutsu & Takahashi, 1997; Newman et al.,
36 1992; Wu et al., 1992), their role in the efficacy of *Panax ginseng* has not been
37 completely elucidated. Recent articles have reported that multiple components in *Panax*
38 *ginseng*, such as lipids, polysaccharides, peptides, and amino acids act synergistically
39 (Spelman, Burns, Nichols, Winters, Ottersberg & Tenborg, 2006; Zeng, Liang, Jiang,
40 Chau & Wang, 2008). Therefore, to elucidate the efficacy of this herb, simultaneous
41 analysis of the secondary-metabolite complexes of relatively small molecules like
42 ginsenosides is very important.

43 Mass spectrometry (MS) is a powerful technique used to analyze metabolites in
44 biological samples and tissues. It can be used to directly and simultaneously detect
45 multiple components in crude samples such as TCM products. Although MS combined

ACCEPTED MANUSCRIPT

ACCEPTED MANUSCRIPT

46 with liquid chromatography (LC) and gas chromatography (GC) can be used to analyze
47 ginsenosides (Cui, Song, Liu & Liu, 2001; Fuzzati, Gabetta, Jayakar, Pace & Peterlongo,
48 1999; Li, Mazza, Cottrell & Gao, 1996; Tawab, Bahr, Karas, Wurglics &
49 Schubert-Zsilavecz, 2003; Wang et al., 2008), these techniques are time consuming
50 (analysis time, ~30 min.). Matrix-assisted laser desorption/ionization (MALDI) MS is a
51 soft and sensitive ionization technique that uses chemical matrices such as
52 4-hydroxy-α-cinnamic acid (CHCA), 2,5-dihydroxybenzoic acid (DHB), and sinapic
53 acid (SA) to facilitate ionization of the analyte. However, one of the main problems of
54 MALDI-MS is the overlapping of the matrix peaks and fragment peaks in the low-mass
55 region (m/z ~ 800). These shortcomings significantly complicate the application of these
56 techniques in the multiple-component analysis of samples such as TCM products and
57 their metabolites. It is our approach that these shortcomings can be overcome by using
58 advanced analytical techniques developed through interdisciplinary collaboration.

59 Nanomaterials have shown great potential in facilitating the development of new
60 technologies (Chithrani & Chan, 2007; Moritake et al., 2007; Taira, Hatanaka, Moritake,
61 Kai, Ichiyanagi & Setou, 2007). Nanoparticles (NPs) have been used in the
62 development of solar cells (Kitada, Kikuchi, Ohono, Aramaki & Maenosono, 2009),
63 sensors (Ai, Zhang & Lu, 2009; Kalogianni, Koraki, Christopoulos & Ioannou, 2006),

ACCEPTED MANUSCRIPT

ACCEPTED MANUSCRIPT

64 catalysts (Mitsudome, Noujima, Mizugaki, Jitsukawa & Kaneda, 2009), drug delivery
65 systems (Moritake et al., 2007), and imaging techniques (Taira, Sugiura, Moritake,
66 Shimma, Ichiyanagi & Setou, 2008). However, there have been very few studies on the
67 use of NPs in food chemistry (Ravindranath, Mauer, Deb-Roy & Irudayaraj, 2009; Yang,
68 Kostov, Bruck & Rasooly, 2009). Previous studies used photospectroscopy with NPs to
69 detect analytes; however, this technique afforded limited detection of the multiple
70 components in food. In our previous reports, to obtain ionization-assisting agents that
71 could be used to perform nanoparticle-assisted laser desorption/ionization
72 (nano-PALDI) MS without significantly increasing the background signals, we prepared
73 metal oxide nanoparticles surrounded by amorphous SiO_2 and an amino group (Figure 1
74 c and d) (Moritake, Taira, Sugiura, Setou & Ichiyanagi, 2009; Taira, Kitajima,
75 Katayanahi, Ichiishi & Ichiyanagi, 2009; Taira et al., 2008). Here, we investigated the
76 suitability of nano-PALDI MS for analyzing lipid and ginsenosides in *Panax ginseng*
77 extracts. We assessed the ionization of several standard ginsenosides by using
78 nano-PALDI MS as an analysis marker for crude samples. Further, we used the
79 nano-PALDI MS technique to separate and evaluate the original ingredients in the
80 complicated MS spectrum for ginseng extract.

81 **Method**

ACCEPTED MANUSCRIPT

ACCEPTED MANUSCRIPT

82 Materials

83 Standard ginsenosides (Rb_1, Rb_2, Rc, Rd, Re, Rf, and Rg_1 with purity >98 %, >94%,
84 >99%, >99%, >99%, >99%, and >99%, respectively) were purchased from Funakoshi
85 (Tokyo, Japan). The extract was obtained from tissue-cultured *Panax ginseng* (TCPG)
86 (Nitto Denko, Osaka, Japan). The TCPG powder was extracted using hot water (80°C)
87 for 2 h, dried, and re-extracted with 70% (v/v) methanol. The extract thus obtained was
88 applied to a small column (Sep-Pak cartridge C18 and NH_2; Waters, Milford, USA) to
89 concentrate the ginsenosides.

90

91 Preparation of nanoparticles

92 Manganese oxide-based nanoparticles were prepared by mixing aqueous solutions
93 of $MnCl_2 \cdot 4H_2O$ (5 ml, 100 mM; WAKO Pure Chemicals, Japan) and
94 3-aminopropyltriethoxysilane (5 ml; γ-APTES; Shinetsu, Kagaku, Japan). After stirring
95 at room temperature for 1 h, the resulting precipitate was washed several times with
96 ultrapure water and dried at 55°C in an incubator. The dried samples were pulverized in
97 a porcelain mortar. The morphology and diameter distribution of the nanoparticles were
98 investigated using a transmission electron microscope (TEM; H-7100; Hitachi, Japan).

99

ACCEPTED MANUSCRIPT

ACCEPTED MANUSCRIPT

100 Nano-PALDI mass spectrometry

101 The utility of the nanoparticles as ionization-assisting materials in mass spectrometry
102 was confirmed in a MALDI-TOF-type instrument (TOF = time of flight;
103 Voyager-DE-RP; Applied Biosystems, Germany) by using a N_2 laser with an emission
104 wavelength of 337 nm. Samples of standard ginsenosides samples such as G-Rb_1, G-Rb_2,
105 G-Rc, G-Rd, G-Re, G-Rf, and G-Rg_1 were chosen for the analysis. The nanoparticles (1
106 mg) were dispersed in 1 mL of methanol or in 1 mL of a 10 mM methanolic solution of
107 sodium acetate. Each sample was independently dissolved in distilled water at a
108 concentration of 100 pmol/μL. Each analyte solution (1 μL) was pipetted on to the
109 surface of the nanoparticle-coated target plates. The peptides used for external
110 calibration were deposited on the plate to minimize the mass shift. The analyte surface
111 was irradiated with 100 laser shots in the positive mode.

112

113 Results and discussion

114 Ability of the nanoparticles to assist ionization of pure sample analytes

115 We used the standard ginsenosides G-Rb_1 [exact mass (Me): 1108.6], G-Rb_2 (Me:
116 1078.6), G-Rc (Me: 1078.6), G-Rd (Me: 947.2), G-Re (Me: 947.2), G-Rf (Me: 800.5),
117 and G-Rg_1 (Me: 800.5) to evaluate the usefulness of employing nanoparticles as laser

ACCEPTED MANUSCRIPT

ACCEPTED MANUSCRIPT

118 desorption/ionization materials. The mass spectra of the standard ginsenosides were
119 obtained in the presence of nanoparticles with sodium ions, thereby ensuring that the
120 precursor ions were obtained in the form of $[M + Na]^+$ ions (Taira et al. 2008). In this
121 study, the standard ginsenosides formed sodium-adduct ions and yielded high-intensity
122 signals. Further, to characterize a variety of ginsenosides, we performed post-source
123 decay (PSD) MS for structural analysis.

124 For G-Rb_1, we obtained a precursor $[M + Na]^+$ ion at *m/z* 1132.1. This ion yielded
125 fragment ions $[z1 + Na]^+$ (at *m/z* 789.3), which corresponded to the combination of the
126 agricone moiety and disaccharide moiety of R_1 or R_2, and $[y1 + Na]^+$ (at *m/z* 364.7),
127 which corresponded to the disaccharide moiety of R_1 or R_2 (Figure 2a).

128 Similarly, the PSD spectra of G-Rb_2 and Rc showed a precursor ion at *m/z* 1102.1 and
129 the 2 derivative ions, namely, $[y1 + Na]^+$ at *m/z* 335.2, which corresponded to the
130 disaccharide moiety of R_1, and $[z1 + Na]^+$ at *m/z* 789.8 (Figure 2b) and 789.6 (Figure 2c),
131 which corresponded to the combination of the agricone and disaccharide moieties of R_2.

132 For G-Rd, we obtained an $[M + Na]^+$ ion at *m/z* 970.1 and 3 fragment ions at *m/z*
133 789.3, 365.2, and 203.1. The fragment ion $[z1 + Na]^+$ at *m/z* 789.3 corresponds to an R_1
134 molecule without the glucose moiety. The *m/z* values for the smaller fragment ions $[y2 + Na]^+$
135 and $[y1 + Na]^+$ (365.2 and 203.1, respectively) were consistent with the

ACCEPTED MANUSCRIPT

136 molecular masses of sodium-adducted disaccharide and glucose moieties from R_2 and R_1,

137 respectively (Figure 2d).

138 For G-Re (*m/z* of the precursor ion, 970.1), we obtained 2 fragment ions $[z1 + Na]^+$

139 and $[y1 + Na]^+$ at *m/z* values 789.2 and 203.1, respectively. The mass difference

140 between the precursor ion and the fragment ion at *m/z* 789.2 was 180.9, which indicated

141 the loss of a glucose molecule. The fragment ion at *m/z* 203.1 indicated a

142 sodium-adducted glucose moiety from R_1 (Figure 2e). The same exact mass of R_f and

143 Rg_1 showed difference in the PSD spectra. The PSD of G-Rf showed only 1 fragment

144 ion $[z1 + Na]^+$ at *m/z* 365.2, which corresponded to the disaccharide moiety from R_3

145 (Figure 2f). In contrast, the PSD of G-Rg_1 showed 2 fragment ions, namely, $[z1 + Na]^+$

146 and $[y1 + Na]^+$ at *m/z* values 643.8 and 202.9, respectively, which corresponded to the

147 agricone and glucose moieties of R_1 or R_3 and the divided glucose moiety from R_1 or R_3,

148 respectively (Figure 2g). We distinguished the molecules with the same exact mass on

149 the basis of the differences in the composition of disaccharides (G-Rf) and

150 monosaccharides (G-Rg_1). These nano-PALDI PSD fragmentation patterns were in

151 good agreement with the MALDI PSD fragmentation patterns of standard ginsenosides

152 (data not shown). This finding indicated that our technique could also yield accurate

153 results under mild ionization conditions without unnecessary degradation of the

ACCEPTED MANUSCRIPT

ACCEPTED MANUSCRIPT

154 bioactive molecule. These results could be utilized for analyzing the index of raw
155 sample like plant extracts.
156 We observed a number of high-intensity signals for ginsenosides in the extract of
157 *Panax ginseng* t mass spectra obtained with nanoparticles in the absence (Figure 3a) or
158 presence (Figure 3b) of sodium ions. Although there were few MS signals with
159 intensity greater than *m/z* 600, we could confirm the signals that corresponded to
160 ginsenosides. In the case of the G-Rb_1 ions (*m/z* 1131.6 $[M + Na]^+$; 1147.6 $[M + K]^+$),
161 both sodium- and potassium-adduct ions were observed in the absence of sodium
162 acetate (Figure 3a inset), because the extract originally included salt ions, especially
163 sodium and potassium salts. In the MS spectrum, such salt ions preferentially appeared
164 in their adducted form, rather than the protonated form. However, the related signals
165 showed a convergence only in the case of the sodium-adducted form (*m/z* 1131.2).
166 Interestingly, the correlation between the signals of the sodium-adducted form of
167 G-Rg_1 (*m/z* 823.1) and G-R_{b2} or R_c (*m/z* 1102.1) appeared only in the presence of
168 sodium acetate (10 mM) (Figure 3b inset). In addition, the background noise in the
169 presence of sodium acetate (Figure 3b inset), was lower than in the absence of sodium
170 acetate (Figure 3a inset). The sodium-adducted forms of G-Rg_1 and G-Rb_2 or Rc were
171 more easily ionized than other ion-adducted forms, such as the proton- or

ACCEPTED MANUSCRIPT

ACCEPTED MANUSCRIPT

172 potassium-adducted form. This result indicated that the ginsenosides had optimal
173 ionization forms. Moreover, in the low molecular range (m/z 200–400), the signal
174 intensities in the presence of sodium ions (Figure 3b), were lower than that in the
175 absence of these ions (Figure 3a); thus, the signals in this region indicated a
176 preferential ionization to the protonated form. This technique can be used for accurate
177 and simple analysis of complex mixtures such as foods and nutrients; however, the
178 differences in the ionization characters of these samples must be carefully considered
179 while performing these analyses.

180 To perform structural analysis using post-source decay (PSD) nano-PALDI mass
181 spectrometry, we deduced that the 4 signals at *m/z* 551.5, 823.1, 1102.4, and 1132.1
182 were obtained from the extract of *Panax ginseng* in the presence of sodium ion and
183 determined that these signals originated from lysophosphatidylcholine (LPC)-(1-acyl
184 20:1) ($[M + H]^+$ ion), G-Rg_1 ($[M + Na]^+$ ion), G-Rb_2 or G-Rc ($[M + Na]^+$ ion), and
185 G-Rb_1 ($[M + Na]^+$ ion). For the precursor $[M + H]^+$ ion of LPC-(1-acyl 20:1) at *m/z*
186 551.1, the typical fragment ions $[y1]^+$ and $[z1 + H]^+$ were detected at *m/z* 85.9 and 298.5,
187 respectively; this finding provided information on the trimethylamine moiety and the
188 fatty acid (1-acyl 20:1) in the sequence. The PSD fragment patterns indicated that the
189 promptly obtained lipid fragment ions did not originate from the observed molecular

ACCEPTED MANUSCRIPT

ACCEPTED MANUSCRIPT

190 ions, because the prompt fragmentation occurred immediately after the formation of
191 highly unstable protonated precursor ions (Figure 4a) (Al-Saad, Zabrouskov, Siems,
192 Knowles, Hannan & Hill, 2003).

193 Similarly, the PSD spectra of ginsenosides showed fragment ions similar to those of
194 the standard ginsenosides G-Rg_1, G-Rb_2 or G-Rc, and G-Rb_1. The PSD spectrum of
195 G-Rg_1 showed 2 derivative ions that corresponded to the glucose ions (*m/z* 202.9; $[M +$
196 $Na]^+$) of R_1 or R_2 and the agricone moieties (*m/z* 643.8; $[M + Na]^+$) (Figure 4b).

197 We detected a precursor ion at *m/z* 1102.1 and 2 derivative sodium-adduct ions at *m/z*
198 336.3 and *m/z* 789.0, which corresponded to the disaccharide moiety of R_1 or R_3 and the
199 combination of the disaccharide and agricone moieties of R_1 or R_3, respectively. The
200 difference between G-Rb_2 and G-Rc can be attributed to the arabinose conformation
201 (arabinopyranose for G-Rb_2 and arabinofuranose for G-Rc) within the disaccharide
202 moiety of R_2; this conformation can complicate the distinction between G-Rb_2 and G-Rc
203 using the PSD MS technique (Figure 4c). The corresponding PSD spectrum of G-R_{b1} is
204 shown in Figure 4d. We detected an $[M + Na]^+$ precursor ion at *m/z* 1132.1 and 2
205 fragment ions, namely, $[M + Na]^+$ at *m/z* 788.4 and $[M + Na]^+$ at *m/z* 365.0. These
206 fragment ions could be considered as the z1 and y1 ions, which are characteristic of the
207 cleavage of the glycosidic bonds at R_1 or R_2.

ACCEPTED MANUSCRIPT

ACCEPTED MANUSCRIPT

208 These fragment patterns were in good agreement with the PSD spectra of standard
209 ginsenosides (Figure 2 a, b, c, and g). We could identify the bioactive components such
210 as ginsenosides and lipids from the extract by using the nano-PALDI MS technique.
211

212 **4. Conclusions**

213 Nano-PALDI MS allowed ionization and background-free analysis of the small
214 molecules in a *Panax ginseng* extract. The nanoparticles could ionize the standard
215 ginsenosides in the presence of external sodium ions. The obtained signals corresponded
216 to those of sodium-adduct ions. Although conventional matrices do not ionize the
217 analyte in the presence of external salt ions, this technique can facilitate the analysis of
218 crude samples like plant extracts. Using this technique, we detected lipids and
219 ginsenosides in the *Panax ginseng* extract and identified the optimal ion forms of these
220 compounds. We mainly focused on using nano-PALDI MS to investigate the role of
221 ginsenosides as the active components of *Panax ginseng*. However, the contributions of
222 other compounds, such as saccharides, peptides, and proteins, should be investigated.
223 The nano-PALDI MS technique is a good substitute for MALDI and has great potential
224 for rapid screening of bioactive ingredients such as ginsenosides in plant extracts;
225 however, further studies are required to establish their traceability in foods and nutrient

ACCEPTED MANUSCRIPT

ACCEPTED MANUSCRIPT

226 product.

227 In addition, the nanoparticles may be utilized in the mass spectrometric analyses of
228 biomedical tissues (Taira et al., 2008) and in cellular analysis (Moritake et al., 2009).
229 The nanoparticle-based approach used in this study can be employed for simple and
230 efficient identification of various ingredients of foods and herbal products used in TCM.

231

232 **Acknowledgments**

233 We thank member of Takagi and Takamura laboratory in JAIST, particularly Prof. M.
234 Takagi and Prof. Y. Takamura, Ms. A. Makino and Ms T. Taniho for providing technical
235 assistance and advice. This research was supported by a WAKATE-B grant from the
236 Japan Society for the Promotion of Science to S. T. and a Grant-in-Aid to S. T. from
237 JAIST and the resource of coordinated research program to Nitto Denko and a A-STEP
238 to S. T. and Y. S. from Japan Science and Tech. Agency

239

240 **Figure legends**

241 Figure 1

242 A schematic illustration of nanoparticle-assisted laser desorption/ionization
243 (nano-PALDI) mass spectrometry (a). Transmission electron microscopy (TEM) image
244 of the nanoparticles (b). When reserpine (100 pmol) was used as a model drug with the
245 nanoparticles, the nano-PALDI mass spectra (c) did not show any background

ACCEPTED MANUSCRIPT

ACCEPTED MANUSCRIPT

246 interference in the low-mass region. In contrast, the mass spectra of reserpine with
247 4-hydroxy-α-cinnamic acid (CHCA) showed background noise in the low-mass region
248 (d).

249

250 Figure 2

251 The post-source decay nanoparticle-assisted laser desorption/ionization (nano-PALDI)
252 mass spectra of the standard ginsenosides G-Rb_1 (a), G-Rb_2 (b), G-Rc (c), G-Rd (d),
253 G-Re (e), G-Rf (f), and G-Rg_1 (g). The abbreviations for the sugar moieties are glc
254 (β-D-glucose), arap (α-L-arabinose; pyranose), araf (α-L-arabinose; furanose), and rha
255 (α-L-rhamnose).

256

257 Figure 3

258 Mass spectra of the extract with nanoparticles (NPs) alone (a) and with NPs in the
259 presence of sodium acetate (NaAc: 10 mM) (b). The superimposed spectra of
260 tissue-cultured *Panax ginseng* (TCPG) extract with NPs in the absence (upper) and
261 presence of (lower) additional NaAc.

262

263 Figure 4

ACCEPTED MANUSCRIPT

ACCEPTED MANUSCRIPT

264 The post-source decay nanoparticle-assisted laser desorption/ionization (nano-PALDI)
265 mass spectra of lysophosphatidylcholine (LPC)-(1-acyl 20:1) (a), ginsenoside (G)-Rg_1
266 (b), G-Rb_2 or G-Rc (c), and (G)-Rb_1 (d). The abbreviations for the sugar moieties are the
267 same as those used in Figure 2.

268

269 References

270 Ai, K., Zhang, B., & Lu, L. (2009). Europium-based fluorescence nanoparticle sensor for
271 rapid and ultrasensitive detection of an anthrax biomarker. *Angewandte Chemie.*
272 *International Ed. In English*, *48*(2), 304-308.
273 Al-Saad, K. A., Zabrouskov, V., Siems, W. F., Knowles, N. R., Hannan, R. M., & Hill, H. H., Jr.
274 (2003). Matrix-assisted laser desorption/ionization time-of-flight mass spectrometry of
275 lipids: ionization and prompt fragmentation patterns. *Rapid Communications in Mass*
276 *Spectrometry*, *17*(1), 87-96.
277 Chithrani, B. D., & Chan, W. C. (2007). Elucidating the mechanism of cellular uptake and
278 removal of protein-coated gold nanoparticles of different sizes and shapes. *Nano Lett*, *7*(6),
279 1542-1550.
280 Cui, M., Song, F., Liu, Z., & Liu, S. (2001). Metal ion adducts in the structural analysis of
281 ginsenosides by electrospray ionization with multi-stage mass spectrometry. *Rapid*
282 *Communications in Mass Spectrometry*, *15*(8), 586-595.
283 Fuzzati, N., Gabetta, B., Jayakar, K., Pace, R., & Peterlongo, F. (1999). Liquid
284 chromatography-electrospray mass spectrometric identification of ginsenosides in Panax
285 ginseng roots. *Journal of Chromatography A*, *854*(1-2), 69-79.
286 Hijikata, Y., Miyamae, Y., Takatsu, H., & Sentoh, S. (2007). Two Kampo medicines,
287 Jidabokuippo and Hachimijiogan alleviate sprains, bruises and arthritis. *Evidence-Based*
288 *Complementary and Alternative Medicine*, *4*(4), 463-467.
289 Kalogianni, D. P., Koraki, T., Christopoulos, T. K., & Ioannou, P. C. (2006).
290 Nanoparticle-based DNA biosensor for visual detection of genetically modified organisms.
291 *Biosensors and Bioelectronics*, *21*(7), 1069-1076.
292 Kitada, S., Kikuchi, E., Ohono, A., Aramaki, S., & Maenosono, S. (2009). Effect of diamine
293 treatment on the conversion efficiency of PbSe colloidal quantum dot solar cells *Solid State*
294 *Communications*, *149*(41-42), 1853-1855.

ACCEPTED MANUSCRIPT

ACCEPTED MANUSCRIPT

295 Li, T. S. C., Mazza, G., Cottrell, A. C., & Gao, L. (1996). Ginsenosides in roots and leaves of
296 American ginseng. *Journal of Agricultural and Food Chemistry*, *44*(3), 717-720.
297 Metori, K., Furutsu, M., & Takahashi, S. (1997). The preventive effect of ginseng with
298 du-zhong leaf on protein metabolism in aging. *Biological and Pharmaceutical Bulletin*, *20*(3),
299 237-242.
300 Mitsudome, T., Noujima, A., Mizugaki, T., Jitsukawa, K., & Kaneda, K. (2009). Supported
301 gold nanoparticle catalyst for the selective oxidation of silanes to silanols in water. *Chem*
302 *Commun (Camb)*(35), 5302-5304.
303 Moritake, S., Taira, S., Ichiyanagi, Y., Morone, N., Song, S.-Y., Hatanaka, T., Yuasa, S., &
304 Setou, M. (2007). Functionalized Nano-Magnetic Particles for an In Vivo Delivery System
305 *Journal of Nanoscience and Nanotechnology*, *7*(3), 937-944.
306 Moritake, S., Taira, S., Sugiura, Y., Setou, M., & Ichiyanagi, Y. (2009). Magnetic
307 nanoparticle-based mass spectrometry for the detection of biomolecules in cultured cells. *J*
308 *Nanosci Nanotechnol*, *9*(1), 169-176.
309 Newman, M., Wu, J., Gardner, B., Munroe, K., Leombruno, D., Recchia, J., Kensil, C., &
310 Coughlin, R. (1992). Saponin adjuvant induction of ovalbumin-specific CD8+ cytotoxic T
311 lymphocyte responses. *Journal of Immunology*, *148*(8), 2357-2362.
312 Ravindranath, S. P., Mauer, L. J., Deb-Roy, C., & Irudayaraj, J. (2009). Biofunctionalized
313 magnetic nanoparticle integrated mid-infrared pathogen sensor for food matrixes.
314 *Analytical Chemistry*, *81*(8), 2840-2846.
315 Spelman, K., Burns, J., Nichols, D., Winters, N., Ottersberg, S., & Tenborg, M. (2006).
316 Modulation of cytokine expression by traditional medicines: A review of herbal
317 immunomodulators. *Alternative Medicine Review*, *11*(2), 128-150.
318 Sun, S., Wang, C. Z., Tong, R., Li, X. L., Fishbein, A., Wang, Q., He, T. C., Du, W., & Yuan, C.
319 S. (2009). Effects of steaming the root of Panax notoginseng on chemical composition and
320 anticancer activities. *Food Chemistry*, *118*(2), 307-314.
321 Taira, S., Hatanaka, T., Moritake, S., Kai, Y., Ichiyanagi, Y., & Setou, M. (2007). Cellular
322 Recognition of Functionalized with Folic acid Nanoparticles. *e-Journal of Surface Science*
323 *and Nanotechnology*, *5*, 23-28.
324 Taira, S., Kitajima, K., Katayanahi, H., Ichiishi, E., & Ichiyanagi, Y. (2009). Manganese
325 oxide nanoparticle-assisted laser desorption/ionization mass spectrometry for medical
326 applications. *Science and Techonology of Advanced Materials*.
327 Taira, S., Sugiura, Y., Moritake, S., Shimma, S., Ichiyanagi, Y., & Setou, M. (2008).
328 Nanoparticle-assisted laser desorption/ionization based mass imaging with cellular
329 resolution. *Analytical Chemistry*, *80*(12), 4761-4766.
330 Tawab, M. A., Bahr, U., Karas, M., Wurglics, M., & Schubert-Zsilavecz, M. (2003).

ACCEPTED MANUSCRIPT

ACCEPTED MANUSCRIPT

331 Degradation of ginsenosides in humans after oral administration. *Drug Metabl lism and*
332 *Disposition: The Biological Fate of Chemicals*, *31*(8), 1065-1071.
333 Wang, Y. T., You, J. Y., Yu, Y., Qu, C. F., Zhang, H. R., Ding, L., Zhang, H. Q., & Li, X. W.
334 (2008). Analysis of ginsenosides in Panax ginseng in high pressure microwave-assisted
335 extraction. *Food Chemistry*, *110*(1), 161-167.
336 Wu, J., Gardner, B., Murphy, C., Seals, J., Kensil, C., Recchia, J., Beltz, G., Newman, G., &
337 Newman, M. (1992). Saponin adjuvant enhancement of antigen-specific immune responses
338 to an experimental HIV-1 vaccine. *Journal of Immunology*, *148*(5), 1519-1525.
339 Xu, H., & Xu, H. E. (2009). Analysis of trace elements in Chinese therapeutic foods and
340 herbs. *American Journal of Chinese Medicine*, *37*(4), 625-638.
341 Yang, M., Kostov, Y., Bruck, H. A., & Rasooly, A. (2009). Gold nanoparticle-based enhanced
342 chemiluminescence immunosensor for detection of Staphylococcal Enterotoxin B (SEB) in
343 food. *International Journal of Food Microbiology*, *133*(3), 265-271.
344 Zeng, Z. D., Liang, Y. Z., Jiang, Z. H., Chau, F. T., & Wang, J. R. (2008). Quantification of
345 target components in complex mixtures using alternative moving window factor analysis
346 and two-step iterative constraint method. *Talanta*, *74*(5), 1568-1578.
347
348

ACCEPTED MANUSCRIPT

ACCEPTED MANUSCRIPT

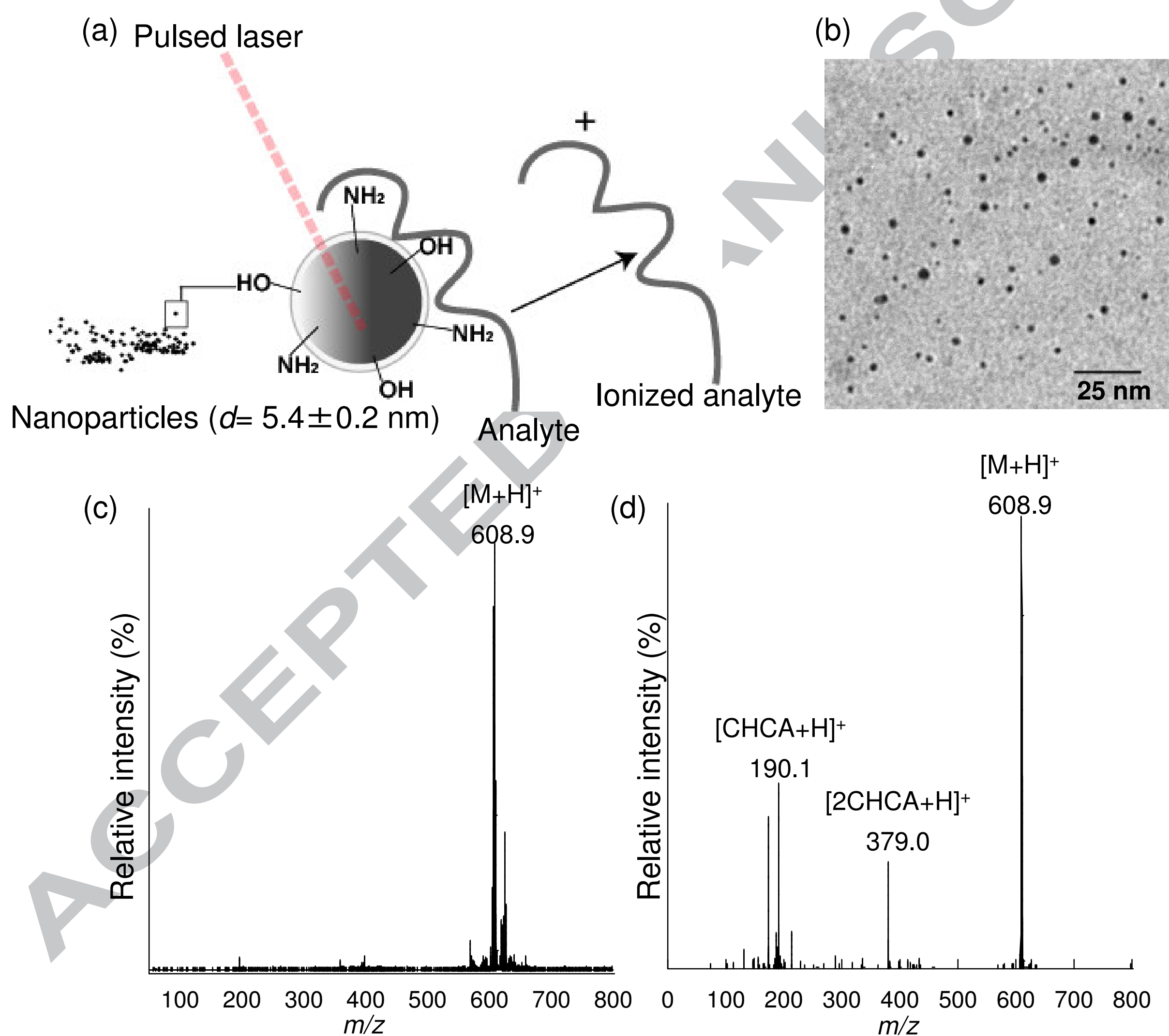

Figure 1 Taira et al.

ACCEPTED MANUSCRIPT

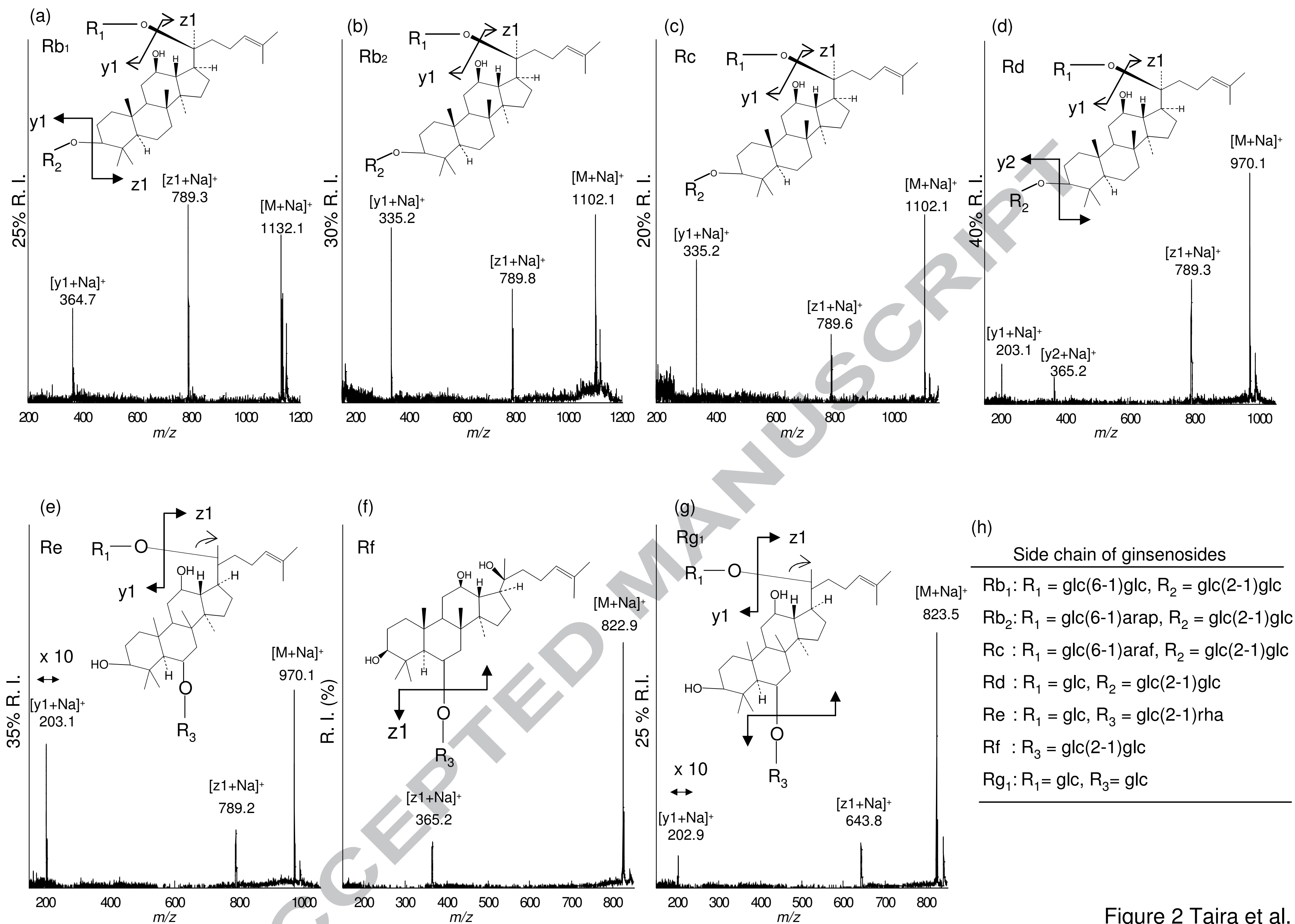

Figure 2 Taira et al.

ACCEPTED MANUSCRIPT

ACCEPTED MANUSCRIPT

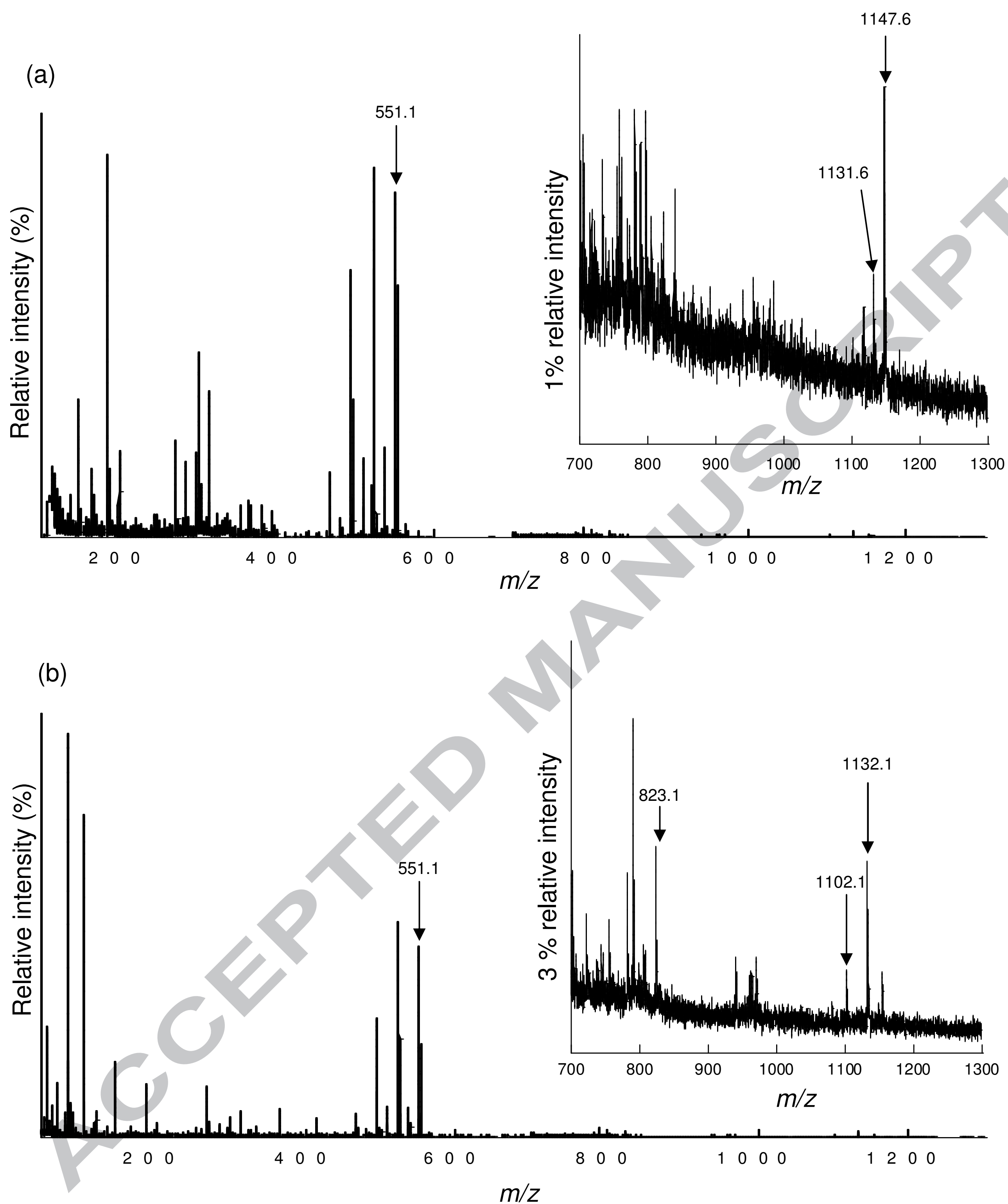

Figure 3 Taira et al.

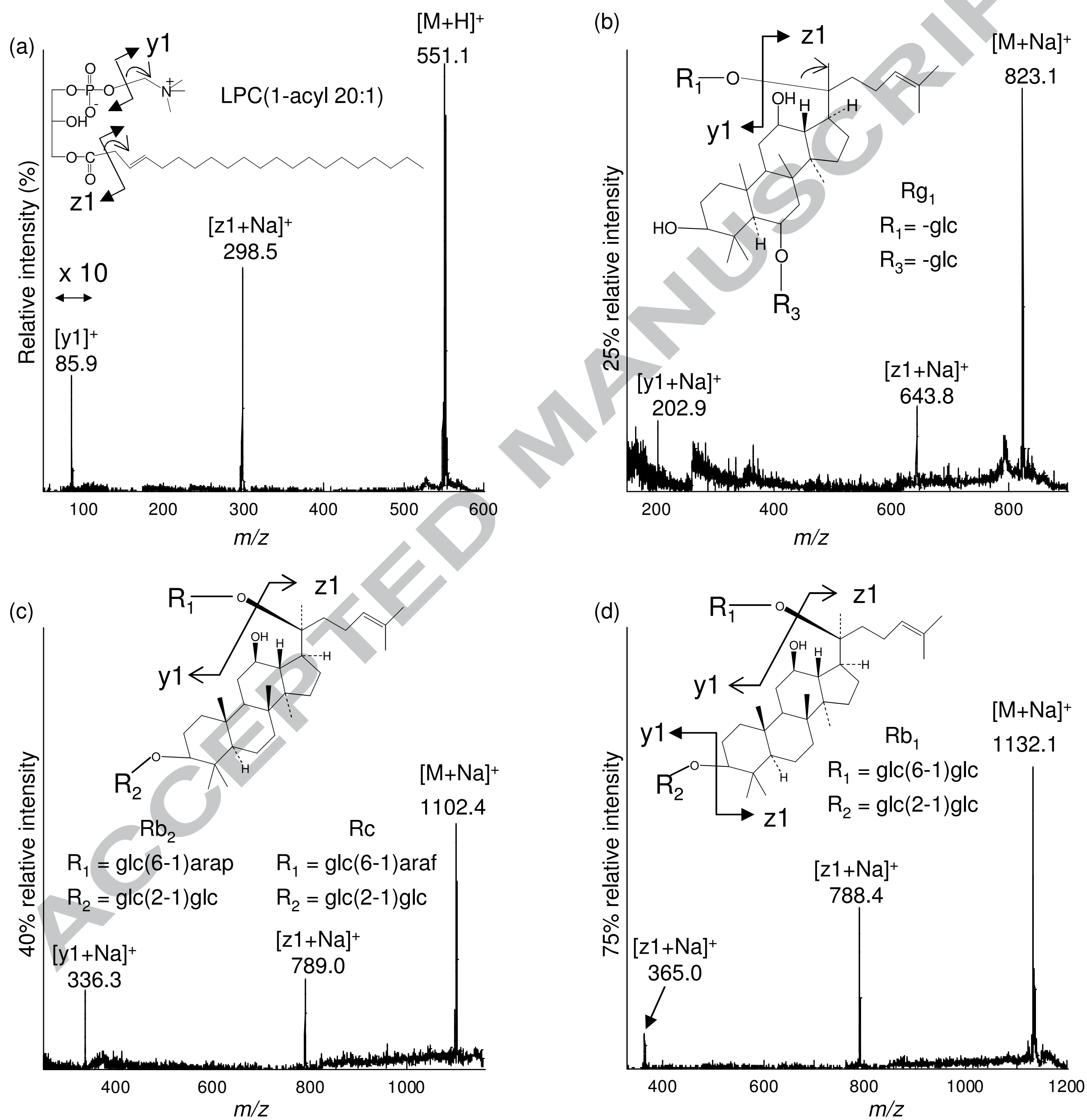

Figure 4 Taira et al.

ACCEPTED MANUSCRIPT